

Kinetic Study of Coniferyl Alcohol Radical Binding to the (+)-Pinoresinol Forming Dirigent Protein[†]

Steven C. Halls, Laurence B. Davin, David M. Kramer, and Norman G. Lewis*

Institute of Biological Chemistry, Washington State University, Pullman, Washington 99164-6340

Received November 3, 2003; Revised Manuscript Received December 31, 2003

ABSTRACT: An essential step in lignan and lignin formation *in planta* is one electron oxidation of (*E*)-coniferyl alcohol (CA) to generate the radical intermediate (CA[•]), which can then undergo directed radical–radical couplings *in vivo*. For lignan formation *in vitro* and *in vivo*, stereoselective coupling of CA[•] only occurs to afford (+)-pinoresinol in the additional presence of (+)-pinoresinol forming dirigent protein (DP). Presented herein is a kinetic and thermodynamic study which reveals the central mechanistic details of the coupling process involved in DP-mediated coupling. DP activity was maximal between pH 4.25 and pH 6.0, with activity being maintained at temperatures below 33 °C. Equilibrium binding assays revealed that coniferyl alcohol was only weakly bound to the DP, with a K_D of $370 \pm 65 \mu\text{M}$. On the other hand, the enantiomeric excess of (+)-pinoresinol formed was dependent on both DP concentration and rate of CA oxidation and, thus, on apparent steady-state [CA[•]]. The data obtained could best be explained using a kinetic model where radical–radical coupling via DP competes with that occurring in open solution. Using this model, an apparent K_M of about 10 nM was estimated from the saturation behavior of (+)-pinoresinol formation with respect to apparent steady-state [CA[•]]. These data strongly suggest that CA[•], rather than CA, is the substrate for DP, in agreement with earlier predictions. A mechanism of directed radical–radical coupling, where two coniferyl alcohol radical substrates are bound per protein dimer, is proposed.

The (*E*)-coniferyl alcohol (**1**) derived lignan (+)-pinoresinol (**4a**, Scheme 1) is a central precursor of many 8–8'-linked plant lignans, which are considered to be deployed primarily in plant defense (*1*). This entry point to the pathway was demonstrated to result from stereoselective coupling of two (*E*)-coniferyl alcohol derived radicals (**2**) in the presence of a dirigent protein (DP)¹ (Scheme 1), whose name was coined to describe its mode of action (Latin: *dirigere*, to guide or align) (*1–4*). This transformation apparently involves two separate reactions (*2*). The first is that of single electron oxidation of coniferyl alcohol (**1**) affording the corresponding radical species (**2**), which in open solution can undergo nonspecific coupling to yield the racemic products (**3–5**, Scheme 1). The second, in the presence of the (+)-pinoresinol forming DP, is that of stereoselective radical–radical coupling to form a single product, (+)-pinoresinol (**4a**, Scheme 1).

The (+)-pinoresinol forming DP has been isolated (*2*) and its corresponding gene cloned (*3*). While the latter encodes a predicted protein of ~18.3 kDa (*3*), posttranslational glycosylation gives a native monomer whose molecular mass

is ca. 24.5 kDa (*5*). Additionally, the protein exists as a homodimer and is predominantly of β -sheet structure. To date, there are over 50 other unique cDNAs, EST's, and genetic sequences in the databases with >70% homology and >40% identity to the (+)-pinoresinol forming DP. Some of these genes are expressed in response to both fungal (*6, 7*) and viral (*8*) pathogen elicitation, thus giving further indirect support to the role of lignans in defense responses.

Although this specific 8–8' coupling mode is found in a particular subset of lignans, it has been proposed that distinct DP and DP-like proteins exist and function for other coupling reactions giving lignans with different linkage types (*1, 9–11*). Moreover, the biosynthesis of other phenolic compounds, such as the biopolymeric lignins (*12*) and the phenolic portion of suberins (*13*), as well as those of insect cuticle melanization and sclerotization, and formation of phenolic polymers in fungal fruiting bodies (*14*) also involve bimolecular phenoxy radical coupling; hence, control of their assemblies may similarly be envisaged to utilize proteins containing dirigent sites, proteins harboring arrays of dirigent sites, or functional analogues thereof (*4, 9*).

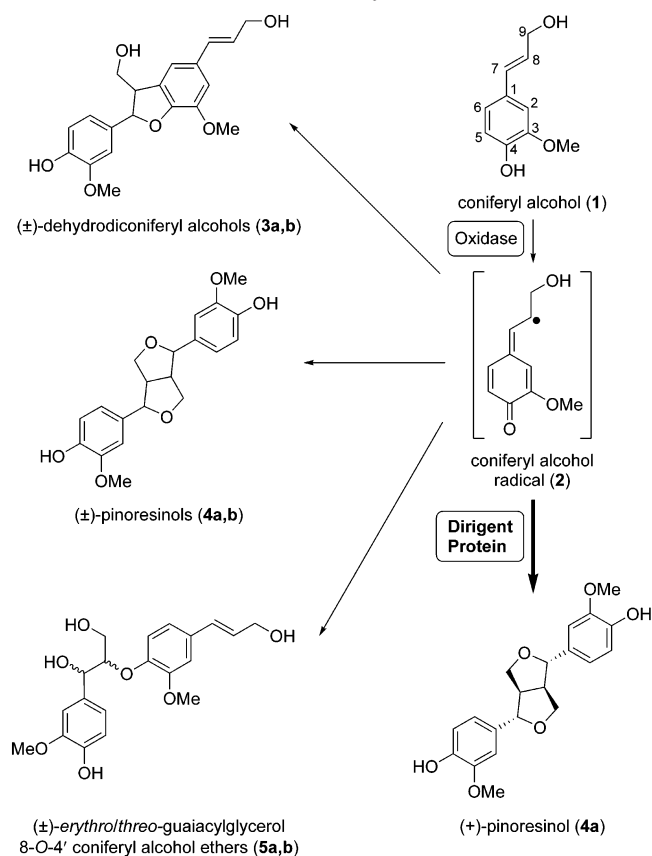
On the basis of our current understanding, the (+)-pinoresinol forming DP appears to use coniferyl alcohol derived radical species (**2**) as substrate, since the DP alone has no demonstrable capacity to oxidize (*E*)-coniferyl alcohol (**1**). *In vitro*, formation of coniferyl alcohol derived radicals (**2**) can be achieved through action of any of a number of one-electron oxidases/oxidants, including laccase, peroxidase, ammonium peroxydisulfate, and FMN radical generating

[†] This research was supported in part by the National Science Foundation (MCB-9976684), the U.S. Department of Energy (DE-FG03-97ER20259), and the Lewis B. and Dorothy Cullman and G. Thomas Hargrove Center for Land Plant Adaptation.

* Address correspondence to this author. Telephone: (509) 335-8382. Fax: (509) 335-8206. E-mail: lewisn@wsu.edu.

¹ Abbreviations: DP, dirigent protein; EST, expressed sequence tag; FMN, flavin mononucleotide; HEPES, *N*-(2-hydroxyethyl)piperazine-*N'*-2-ethanesulfonic acid; Mes, 2-(*N*-morpholino)ethanesulfonic acid.

Scheme 1: Formation of Dirigent Protein Mediated (Stereoselective) versus Nonspecific (Racemic) Coupling Products of Coniferyl Alcohol Radicals (2), Following One-Electron Oxidation of Coniferyl Alcohol (1)^a



^a Redrawn from ref 5.

systems (2). However, no precise physiological role for any of these (oxidases and/or oxidants) has yet been identified for the *in vivo* formation of (+)-pinosresinol (4a).

In the absence of the DP, the coniferyl alcohol radical species (2) (generated using, for example, FMN or laccase) combine in open solution *in vitro* to afford (±)-dehydrodiconiferyl alcohols (3a/b), (±)-pinosresinols (4a/b), and *erythro/threo*-(±)-guaiacylglycerol coniferyl alcohol ethers (5a/b) in ratios of ~1:0.5:0.3, respectively (2) (Scheme 1). The measured rate constant for second-order coupling of the coniferyl alcohol radical (2) species in open solution (aqueous, pH 7.8 and 13.0, 22 °C) has been estimated as $(5.7 \pm 3.0) \times 10^8 \text{ M}^{-1} \text{ s}^{-1}$ (15), this in turn representing a value approaching the diffusion limit. Interestingly, radical–radical coupling results in formation of quinone–methide intermediates (Scheme 2A) (15), which can then undergo nucleophilic attack by solvents (such as H₂O) or intramolecular cyclization to afford the corresponding lignans (3–5), respectively. The overall rates of the quinone–methide to phenol transitions for these molecular species have been reported as being relatively slow, with an estimated average rate constant of $5.78 \times 10^{-3} \text{ s}^{-1}$ at 23 °C (16) for the three dimers (3–5, Scheme 2A). (On the other hand, the precise intramolecular cyclization rates leading to both 3a/b and 4a/b have not been determined; these, however, are presumably of a somewhat faster average rate constant than the reaction leading to the formation of 5a/b due to the proximity of the hydroxyl groups facilitating intramolecular ring closure.)

Previous time course studies of coniferyl alcohol (1) oxidation, in the presence of the dirigent protein, have shown that the DP was capable of almost exclusively producing (+)-pinosresinol (4a) at essentially the same rate as formation of the racemic dimers 3–5 in the absence of DP (2). Thus, since it has been previously established that coniferyl alcohol radicals (2) combine in a near-diffusion-limited reaction (15, 17), it can be provisionally envisaged that the DP competes for the same radical species in a near-diffusion-limited reaction as well. However, interactions between DP and coniferyl alcohol (1) may also occur. In this study (see below), these potential interactions were examined through the use of equilibrium dialysis experiments.

Preliminary apparent K_M values for coniferyl alcohol (1) were previously reported for the DP ($10 \pm 6 \text{ mM}$) in the presence of fungal laccase ($0.100 \pm 0.003 \text{ mM}$), FMN ($0.10 \pm 0.01 \text{ mM}$), and a co-isolated plant laccase ($1.6 \pm 0.3 \text{ mM}$) (2). However, the data obtained represented only apparent K_M values since the actual rate-limiting processes had not yet been determined: i.e., the data could not distinguish between the various processes (including which step was rate limiting) involved in generating (+)-pinosresinol (4a), such as oxidation, binding of the corresponding substrate(s) (i.e., one or two), or the control of stereospecific coupling and subsequent intramolecular cyclization.

This investigation thus further analyzes the kinetics of (+)-pinosresinol (4a) formation in the presence of the DP, including an examination of effects of temperature and pH on overall activity (conversion). Of particular interest is the interrelationship between DP concentration and the presumed steady-state radical concentration on the rate of total dimer production and on DP-mediated (+)-pinosresinol (4a) formation.

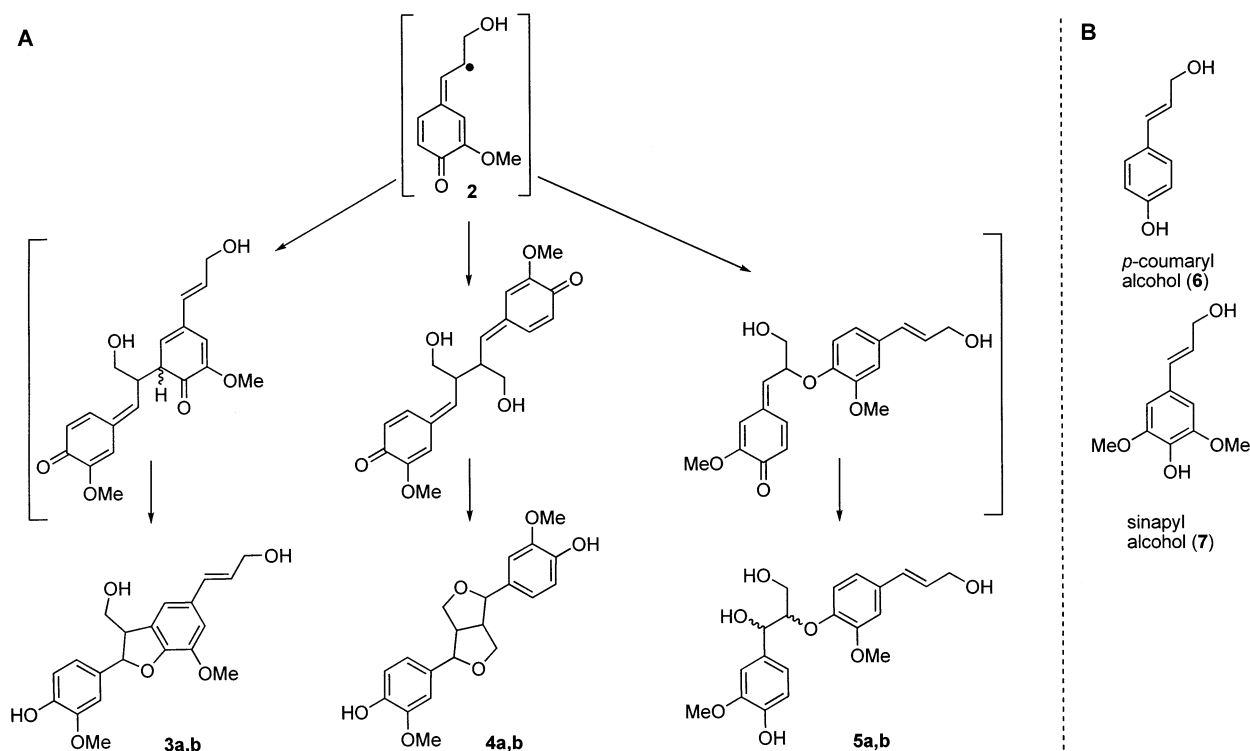
MATERIALS AND METHODS

DP Assay. The DP was purified as described earlier (5) with assay conditions modified from Davin et al. (2) as follows: DP (40 nM, homodimer), FMN (1 mM), HEPES–Mes–sodium acetate buffer (33 mM, pH 5.0), Na₂SO₄ (75 mM), and (*E*)-[9-³H]coniferyl alcohol (1) (4 mM, 7 MBq mol⁻¹ L⁻¹) (the reaction initiator) in a total volume of 250 μL were incubated for 4 h at 30 °C in a shaking (1 Hz) water bath, with the whole being illuminated by fluorescent room lighting. The assay products were subjected to sequential reversed-phase Chiralcel OD HPLC analyses (2), with corresponding controls (assays in the absence of DP, FMN, or both) being carried out.

Temperature Optima and Stability of (+)-Pinosresinol Forming DP. Assay conditions as above were carried out, but at various temperatures: 4, 10, 15, 18, 25, 28, 30, 33, 36, 40, 45, 50, 55, and 60 °C, respectively. The thermal stability of the DP was also examined by incubation of the assay mixture [all constituents of the DP reaction assay, without coniferyl alcohol (1), in 200 μL] at 40, 45, 50, 55, 60, 65, and 70 °C, respectively, for 30 min. The temperature was then lowered to 30 °C, with individual assays being initiated by addition of coniferyl alcohol (1) (50 μL, 20 mM) and incubated for 4 h as above.

pH Optima and Stability of (+)-Pinosresinol Forming DP. The DP reaction assay conditions were followed as above, except for employment of a four-component buffer of maleic

Scheme 2: (A) Formation of (±)-Dehydrodiconiferyl Alcohols (8–5') (**3a,b**), (±)-Pinoresinols (8–8') (**4a,b**), and *erythro*/*threo*-(±)-Guaiacylglycerol-8-*O*-4'-Coniferyl Alcohol Ethers (8-*O*-4') (**5a,b**) Linked Dimers via Quinone–Methide Intermediates, and (B) Monolignols (**6**) and (**7**)



acid, acetic acid, Mes, and HEPES (33 mM each) at pH values ranging from 3 to 8 in 0.25 pH unit increments. The pH stability of the DP between pH 3 and pH 10 was also investigated: assay mixtures (150 μ L) [with Na₂SO₄ (75 mM), without coniferyl alcohol (**1**)] were first incubated at each pH value (from 3.0 to 10.0 in 0.25 pH increments) for 30 min, following which the pH was adjusted to pH 5.0 by addition of an empirically determined concentration of either NaOH or H₂SO₄ (50 μ L), following which assays were immediately initiated by addition of coniferyl alcohol (**1**) (50 μ L, 20 mM) as above.

Effects of Varying DP Concentration. Assays were carried out using DP assay conditions, as above, except for varying the concentration of the DP homodimer (i.e., from 10, 20, 40, 80, 160, 320, to 640 nM), respectively.

Variation in Oxidative Capacity. Assays were carried out using DP assay conditions, except for varying the oxidative capacity using *Trametes versicolor* laccase (**18**) as oxidizing agent (rather than FMN). The latter was employed at concentrations sufficient to give (*E*)-coniferyl alcohol (**1**) oxidation rates of 12, 19, 37, 55, 59, 69, 85, 96, 120, 140, 175, and 240 nM s⁻¹. Incubation times were adjusted to maintain, at the time of reaction termination, at least 80% of the initial coniferyl alcohol (**1**), the purpose of which was to maintain conditions of approximately steady-state oxidation, i.e., 4 h (12, 19, 37, 55, 59, 69 nM s⁻¹), 2 h (85, 96, 120, 140 nM s⁻¹), and 1 h (175, 240 nM s⁻¹), respectively.

To estimate free [CA[•]] (**2**), the analysis of Hapiot et al. (**15**) was employed, with the rates of reaction of CA[•] (**2**) described using the equation:

$$\frac{d[\text{CA}^{\bullet}]}{dt} = -2k_{\text{dimer}}[\text{CA}^{\bullet}]^2 \quad (1)$$

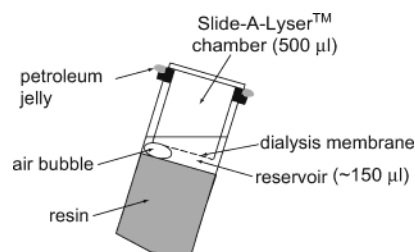


FIGURE 1: Schematic of the equilibrium dialysis chamber.

where $2k_{\text{dimer}}$ is the second-order rate constant for the reaction, previously measured to be $(5.7 \pm 3) \times 10^8 \text{ M}^{-1} \text{ s}^{-1}$ by pulse radiolysis.

Monolignol Binding to DP. Individual solutions (100 μ L), each containing [9-³H]coniferyl alcohol (**1**) at concentrations of 1200, 600, 300, 150, 125, 63, 31, 16, 8, 4, 2, 1, and 0.5 μ M (and a constant radiochemical content of 19.4 MBq mol⁻¹), respectively, in Mes-buffered solution (40 mM, pH 5.0) containing Na₂SO₄ (75 mM) were individually dialyzed against the (+)-pinoresinol forming DP (100 μ L, 300 μ M) in the same buffered solution as follows: Each equilibrium dialysis was performed in a two-chamber cell [modified from Neuhoﬀ et al. (**19**)], custom built from a prewashed (30 min deionized water and then 30 min dialysis buffer) Slide-A-Lyzer cylindrical dialysis chamber (0.1–0.5 mL, 10000 MWCO; Pierce Chemical Co.) inserted in a microcentrifuge tube (2 mL) containing 1.2 mL of preset (polymerized) white acrylic resin (London Resin Co. Ltd., Reading, U.K.). This thus gave a reservoir (of volume ~150 μ L) between the top of the resin and the bottom of the Slide-A-Lyzer insert (Figure 1). The DP-containing solution (100 μ L) was next introduced into the Slide-A-Lyzer compartment with the solution of [9-³H]coniferyl alcohol (**1**) being placed into the reservoir. The contact rims of the two chambers were

then sealed with petroleum jelly to prevent evaporation, and equilibrium dialysis was performed in the device at a 30° axial rotation (5 cycles min⁻¹, 48 h) at 4 °C, after which aliquots (55 µL) were removed from the reservoir for quantification of coniferyl alcohol (**1**) equilibrium concentrations by both liquid scintillation counting and HPLC analyses. Six replicates were performed, as well as six replicates of the equilibrium dialysis system without DP, at each concentration. In addition to coniferyl alcohol (**1**), equilibrium dialysis experiments were performed in the same manner for both unlabeled *p*-coumaryl (**6**) and sinapyl (**7**) alcohols.

From the measured concentrations of unbound [³H]-coniferyl alcohol (**1**), [C]_u, and the known concentrations of total [³H]coniferyl alcohol (**1**), [C]_t, added to the system (confirmed by use of replicates in the absence of DP), the concentrations of bound [³H]coniferyl alcohol (**1**), [C]_b, were determined from the relationship [C]_t = [C]_u + [C]_b. The binding parameters *K*_D and *n* were obtained using the Scatchard equation (20): [C]_b/[C]_u = (*nP*_t - [C]_b)/*K*_D, where *K*_D is the dissociation constant, *n* is the number of identical noninteracting binding sites per molecule, and *P*_t is the total protein concentration.

Kinetic Simulations. Various models of potential relationships between protein, substrate, and product were explored using systems of differential equations describing the kinetics of each individual state. A particular set of equations chosen to describe a plausible model is given in the Discussion. The various kinetic models, or systems of differential equations, were solved using MathCad7 (Mathsoft, Cambridge, MA) software for both steady-state and non-steady-state conditions using the system of equations solution algorithm or the Bulirsch–Stoer method (variation in time resolution was inconsequential), respectively. The rate constants for each system of equations describing the models were determined by iteratively employing the method of steepest descent to find the optimum for each parameter. Goodness of fit for each model was determined by examining the distribution of residuals, particularly the relative distribution of residuals to compensate for the various concentrations of protein. Additionally, the relative mean square deviation of the observed data to the predicted data was used as a measure of fit quality, with the robustness of the reported model tested against known data for initial and boundary values of coniferyl alcohol (**1**), coniferyl alcohol radical (**2**), (+)-pinorensin (**4a**), DP, and incubation time.

RESULTS

Coniferyl Alcohol–DP Binding. Figure 2 shows a Scatchard plot of the [³H]coniferyl alcohol (**1**) bound ([C]_b) fraction versus the ratio of bound/unbound substrate ([C]_b/[C]_u) for 300 µM DP. The best fit obtained is with 2.05 ± 0.17 independent and identical binding sites (*n*) for (*E*)-[³H]coniferyl alcohol (**1**) with the DP homodimer, each with a *K*_D of 370 ± 65 µM. Equilibrium binding assays were also performed with both *p*-coumaryl (**6**) and sinapyl (**7**) alcohols (Scheme 2B); however, no detectable binding of either was detected (*K*_D > 0.5 mM); data not shown.

Competition between DP-Mediated and Unmediated Coupling. Figure 3 shows the effects of increasing DP concentrations on the formation rates of each of the racemic [9,9'-³H]

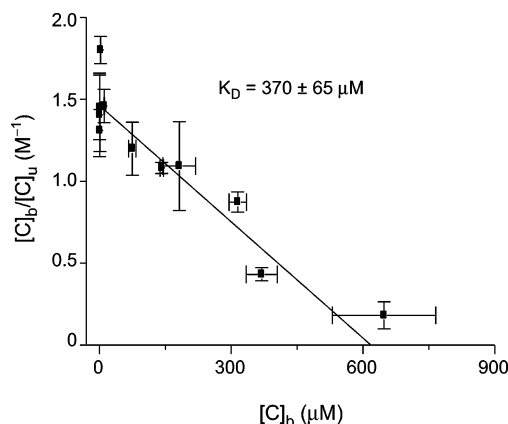


FIGURE 2: Scatchard plot of (*E*)-coniferyl alcohol (**1**) binding to DP (shown with DP at a concentration of 300 µM as an example).

products **3–5** following [³H]CA• (**2**) coupling versus that of (+)-[9, 9'-³H]pinorensin (**4a**) formation in enantiomeric excess. For all concentrations examined, the products so obtained were subjected to reversed-phase HPLC in order to purify each lignan, with radiolabeled amounts of each quantified by liquid scintillation counting. Fractions corresponding to [9,9'-³H]pinorensin (**4**) were subsequently subjected to chiral HPLC analyses to determine the relative ratios of the (+)- and (–)-antipodes **4a/b**.

In the absence of the DP, only racemic [9,9'-³H]lignans (**3–5**) were obtained [i.e., (±)-[9,9'-³H]dehydroconiferyl alcohols (**3a,b**), (±)-[9,9'-³H]pinorensins (**4a,b**), and (±)-[9,9'-³H]erythro/threo-guaiacylglycerol coniferyl alcohol ethers (**5a,b**) in ratios of ~1:0.5:0.3, respectively, as noted earlier (2)]. Increasing the DP concentration had little to no effect on overall coupling rates; i.e., it did not change the rate of dimer production. Instead, it resulted in a progressive increase in stereoselective coupling affording (+)-[9,9'-³H]pinorensin (**4a**) (Figure 3B) with a stoichiometric reduction in the levels of the racemic [9,9'-³H] products **3–5**. The increase in enantiospecificity corresponding to an increase in DP concentration is interpreted as reflecting a competition between unmediated and DP-mediated CA• (**2**) coupling; at DP concentrations >160 nM, the DP-directed coupling essentially out-competes unmediated coupling in open solution.

Temperature and pH Optima. A DP concentration (40 nM) was chosen to examine pH and temperature effects, using the DP reaction assay (Materials and Methods, pH 5.0), with an estimated oxidation rate of coniferyl alcohol (**1**) of 70 nM s⁻¹, this giving (+)-pinorensin (**4a**) in ca. 50% enantiomeric excess. FMN was chosen as a nonenzymatic oxidant since the oxidation of coniferyl alcohol (**1**) had a nearly linear response with increasing temperature from ca. 15 to 35 °C (Figure 4A), i.e., producing a greater oxidation rate with increasing temperature. It was found that a nearly constant 50% enantiomeric excess of (+)-pinorensin (**4a**) was maintained in reactions performed at temperatures ranging between 4 and 33 °C (Figure 4B) under these conditions. On the other hand, the DP appeared to begin to inactivate at temperatures >33 °C, with a steady loss of (+)-pinorensin (**4a**) forming capacity up to 50 °C. A subsequent temperature recovery assay did, however, establish that the DP was capable of recovering full activity, if the temperature did not exceed 45 °C; however, no activity was observed in

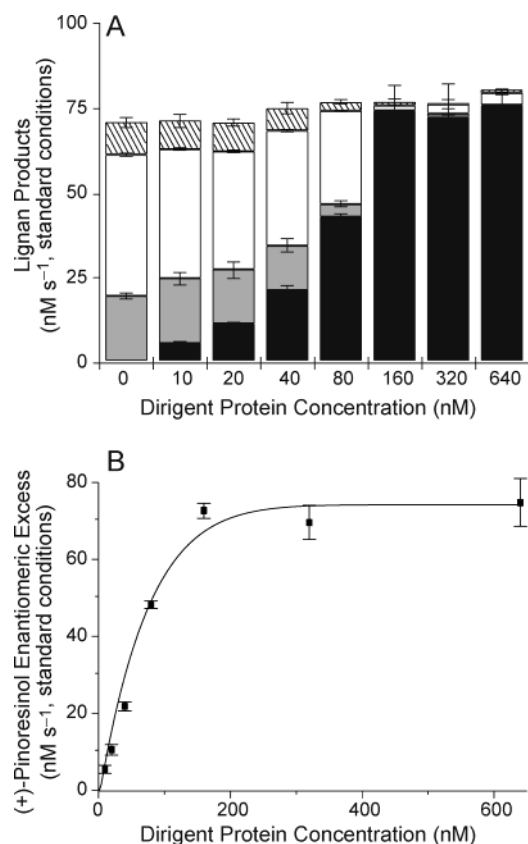


FIGURE 3: Dirigent protein mediated coupling of (*E*)-[9-³H]coniferyl alcohol (**1**). (A) Effect of varying DP concentration on (*E*)-[9-³H]-coniferyl alcohol (**1**) derived coupling product rates under standard assay conditions. Key: black bar, (+)-[9,9'-³H]pinoresinol (**4a**); gray bar, racemic (±)-[9,9'-³H]pinoresinols (**4a,b**); white bar, racemic [9,9'-³H]dehydroconiferyl alcohols (**3a,b**); and hatched bar, racemic [9,9'-³H]erythro/threo-guaiacylglycerol-8-*O*-4'-coniferyl alcohol ethers (**5a,b**). (B) Rate of (+)-[9,9'-³H]pinoresinol (**4a**) being formed in enantiomeric excess with different DP concentrations under standard assay conditions.

solutions exposed to temperatures in excess of 50 °C (data not shown).

Figure 5A shows the small fluctuations in coniferyl alcohol (**1**) oxidation rates as a function of pH during FMN oxidation. The pH-activity profile of (+)-pinoresinol (**4a**) [percent enantiomeric excess (ee)] formation (Figure 5B) revealed that the DP was capable of maximum conversion between pH 4.25 and pH 6.0; this capability, however, rapidly diminished at pH values >6 and <4. Interestingly, while recovery of full capacity was still possible after exposure to pH 8.0, the protein was irreversibly inactivated at a pH <3.75 (data not shown).

DP Reaction Kinetics. For more detailed kinetic analyses, optimized assay conditions were chosen at pH 5.0 and at 30 °C. Figure 6 shows the relationship between the enantiomeric excess of (+)-pinoresinol (**4a**) versus the overall CA (**1**) oxidation reaction rates [as described in Materials and Methods (Variation in Oxidative Capacity)] as both [DP] levels and CA* (**2**) production rates were manipulated. Different concentrations of laccase, rather than FMN, were used in this case to provide different coniferyl alcohol radical (**2**) concentrations, because laccase (or peroxidase) was capable of producing higher concentrations than FMN. The oxidation rate of coniferyl alcohol (**1**) was thus measured in the steady state in terms of twice the sum of formation of

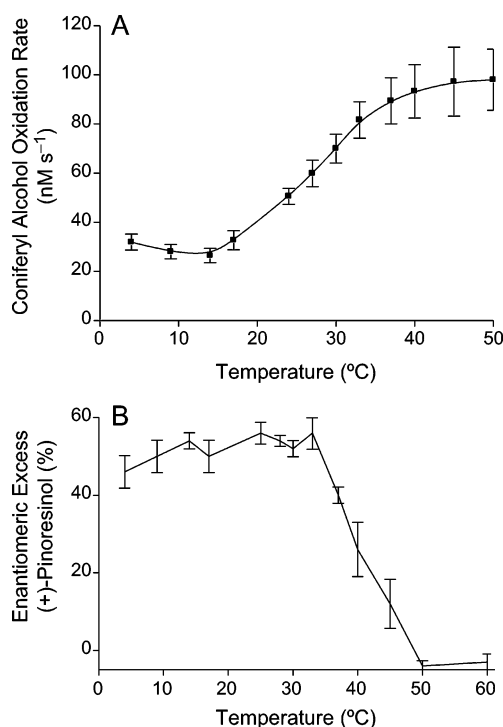


FIGURE 4: Effects of temperature on DP-mediated coupling of (*E*)-coniferyl alcohol radicals (**2**) under standard assay conditions (40 nM DP dimer, pH 5.0). Effects on (A) rate of coniferyl alcohol (**1**) oxidation and (B) enantiomeric excess of (+)-pinoresinol (**4a**) being formed in the presence of FMN.

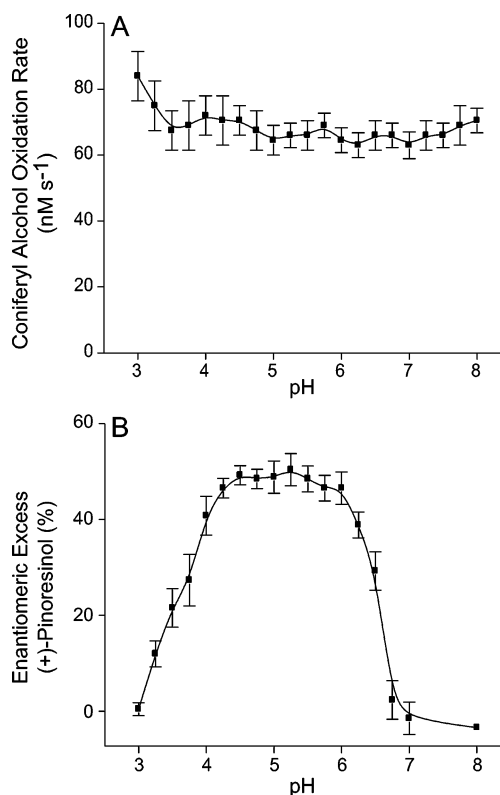


FIGURE 5: Effect of pH on DP activity and coniferyl alcohol (**1**) oxidation rate. (A) Effects on coniferyl alcohol (**1**) oxidation rate in the presence of FMN and (B) effects of pH on DP conversion activity under standard conditions and 40 nM DP dimer, 30 °C.

racemic product and of (+)-pinoresinol (**4a**) in enantiomeric excess. Note, however, that as observed earlier (Figure 3) addition of DP had little effect on CA (**1**) oxidation rates

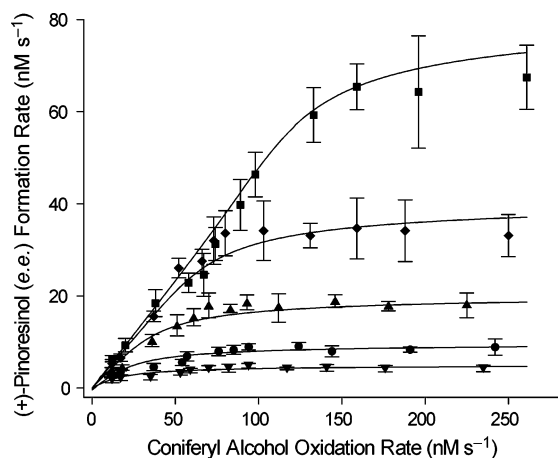


FIGURE 6: Rate of (+)-pinoresinol (**4a**) production in enantiomeric excess, as a function of differential coniferyl alcohol (**1**) oxidation rate using different DP dimer concentrations: (▼) 20 nM, (●) 40 nM, (▲) 80 nM, (◆) 160 nM, and (■) 320 nM. Solid lines indicate model fit to data for each DP concentration; see Discussion.

(data not shown). Interestingly, at each of the coniferyl alcohol (**1**) oxidation rates examined (Figure 6), the fraction of coniferyl alcohol radical (**2**) species coupled by the DP affording (+)-pinoresinol (**4a**) increased with increasing DP concentration until saturation values were achieved, this most likely reflecting accompanying corresponding increases in steady-state $[CA^*]$ (see below). Indeed, the magnitude of the apparent V_{max} was also apparently proportional to the concentration of DP, thereby allowing the direct calculation of the forward rate constant for DP-mediated coupling, k_{fwd} (k_{cat}), as 0.26 ± 0.03 mol for (+)-pinoresinol (**4a**) s^{-1} (mol of DP homodimer) $^{-1}$.

DISCUSSION

The data presented above (Figures 3–6) confirm earlier observations from this laboratory (2) that the DP can specifically direct or guide the stereoselective formation of (+)-pinoresinol (**4a**) from coniferyl alcohol (**1**) versus that of unmediated nonspecific coupling leading to racemic products (**3–5**). The current work further characterizes the kinetics of the process and also addresses two issues: (1) the feasibility that all 8,8'-linked lignan formation *in planta* (e.g., in stems) is DP-mediated and (2) the mechanism of DP-mediated radical coupling.

Kinetic assays of formation of (+)-pinoresinol (**4a**) in enantiomeric excess, using a range of different DP concentrations and CA^* (**2**) production rates (Figure 6), enabled estimation of the k_{cat} of the DP (0.26 ± 0.03 s^{-1} per DP dimer). This is a rather slow rate, though certainly not unprecedented for biosynthetic reactions [i.e., isochorismate pyruvate-lyase, $k_{cat} = 106$ min^{-1} (21); tyrosinase, $k_{cat} = 7.9$ s^{-1} for tyrosine (22); and β -carotene 15,15'-monooxygenase, $k_{cat} = 0.66$ min^{-1} (23); to give just three examples]. An important question that this kinetic data allows us to partially address is whether this DP capacity is both necessary and sufficient for 8,8'-linked lignan production *in planta*. According to Rahman et al. (24), a mature *Forsythia* stem contains approximately 20 mg/g dry weight of 8,8'-lignans, giving approximately 60 μ mol of lignan/g dry weight. Since 1 kg (fresh weight, 430 g dry weight) of *Forsythia intermedia* mature stems contains ca. 2 mg of purified DP (not adjusted

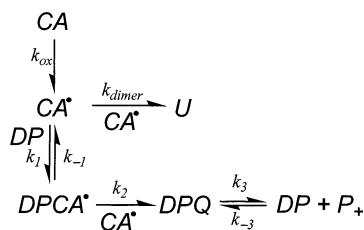
for losses during purification), this gives a lower value estimation of DP > 100 pmol/g dry weight. Thus even at a continuous DP turnover rate of 0.26 s^{-1} , the 8,8'-linked lignans could be produced over a period of about 4 weeks, and most likely considerably shorter. This is well within the time frame for stem growth, and we suggest that, in harmony with proper DP compartmentalization and requisite CA^* (**2**) concentrations, the DP levels observed can sustain all lignan coupling required *in vivo*. In addition, both the temperature and pH dependence of the DP-guided coupling (Figures 4 and 5) appear to be compatible with its proposed role *in vivo*. [The conversion activity of the DP, as measured by the (+)-pinoresinol (**4a**) amounts in enantiomeric excess, was lost at either temperatures above 45 $^{\circ}C$ or at pH < 4, in both instances this likely being a result of irreversible denaturation.]

Independence of CA^* (2**) Formation and the Reaction Catalyzed by DP.** Addition of the DP to the assay mixture had little effect on the overall dimerization rate (Figure 3), this in turn being interpreted as an indication that the DP functions by competing with unmediated coupling following CA^* (**2**) generation. This observation implies (1) that conditions exist during assays where the sum of the rate constants for unmediated and DP-mediated coupling is far greater than that of CA^* (**2**) formation and (2) that the coupling processes are strongly thermodynamically favored (i.e., the reverse reaction is negligible). Together, these would ensure that CA^* (**2**) formation is never product limited under our conditions, and the overall rate of coupling would be determined solely by rate of formation of CA^* (**2**).

Kinetic Mechanism of DP. Three related observations lead to a more detailed view of DP action. The first observation is that CA (**1**) binds only weakly to the DP (K_D of 370 ± 65 μ M; see Figure 2), which tends to discount CA (**1**) as being the true substrate. However, examination of DP-mediated (+)-pinoresinol (**4a**) production as a function of estimated CA^* (**2**) concentration (Figure 6) leads us to conclude that CA^* (**2**) is the direct substrate for the DP with a strong binding constant, as will be explored in more detail below using kinetic simulations. A strong binding constant of the DP toward **2** is not unreasonable, since the protein competes with reactions occurring at rates near the diffusion-controlled limit. Additionally, free $[CA^*]$ (**2**) likely remains very low during the steady-state reaction.

The second observation is that coniferyl alcohol (**1**) has a binding stoichiometry of about two per DP homodimer (Figure 2). While the affinity of coniferyl alcohol (**1**) for the DP is relatively weak (see above), it nevertheless suggests the presence of two binding sites for coniferyl alcohol-like molecules, most likely CA^* (**2**), per homodimer. This is consistent with earlier results from this laboratory demonstrating the homodimeric nature of the active DP complex (5). Furthermore, the fact that only two sites were implicated by the binding studies, coupled with the low K_M with respect to $[CA^*]$ (**2**) for the reaction (see below), strongly argues against any nonspecific effects of DP on coupling.

The third observation of interest is that DP-mediated coupling appears to be quite saturable. In principle, the slow turnover rate would be due to binding of substrate(s), the reaction of bound substrates, or their release. The saturation behavior of the reaction indicates that the rate limitation is in the latter two processes, i.e., that DP interacts strongly

Scheme 3: Proposed Kinetic Model^a

^a Abbreviations: CA, coniferyl alcohol (1); CA*, coniferyl alcohol radical (2); DP, dirigent protein; U, racemic dimers (3–5); DPCA*, dirigent protein–coniferyl alcohol radical complex; DPQ, dirigent protein quinone–methide intermediate complex; P+, DP-mediated (+)-pinoresinol (4a); k_{ox} , rate constant of coniferyl alcohol (1) oxidation; k_2 , rate constant of coniferyl alcohol radical (2) binding to the DPR complex.

with some intermediate in the process, and during the lifetime of this interaction, DP is unable to further process CA* (2). Any intermediates of the coupling reaction or subsequent rearrangements could conceivably be tightly bound or slowly lost and thus account for the slow turnover.

Kinetic Models. In addition to the qualitative observations discussed above, our experiments lend themselves to a quantitative analysis, within the framework of specific kinetic models. Presented here is such an analysis based on what we consider to be the simplest testable model, presented in Scheme 3, and which explains all available data. The system of equations which describe the steady-state model is as follows:

$$d[U]/dt = k_{dimer}[CA^*]^2 \quad (2)$$

$$d[P_+]/dt = k_3[DPQ] - k_{-3}[DP][P_+] \quad (3)$$

$$[DP_{tot}] = [DP] + [DPCA^*] + [DPQ] \quad (4)$$

$$k_1[CA][DP] = k_2[DPCA^*][CA^*] + k_{-1}[DPCA^*] \quad (5)$$

$$k_{ox}[CA^*] + k_{-1}[DPCA^*] = 2k_{dimer}[CA^*]^2 + k_1[CA^*][DP] + k_2[DPCA^*][CA^*] \quad (6)$$

$$k_3[DPQ] + k_{-1}[DPCA^*] = k_1[DP][CA^*] + k_{-3}[P_+][DP] \quad (7)$$

$$k_{-3}[DP][P_+] = k_2[DPCA^*][CA^*] + k_3[DPQ] \quad (8)$$

where [U] is the concentration of the racemic unmediated coniferyl alcohol radical dimerization products (3–5), [P₊] is the concentration of (+)-pinoresinol (4a), [CA] and [CA*] are the concentrations of coniferyl alcohol (1) and its radical species (2), respectively, and [DP], [DPCA*], [DPQ], and [DP_{tot}] are the concentrations of the dirigent protein, the dirigent protein–coniferyl alcohol radical complex, and the dirigent protein–intermediate complex and the combined concentrations of the dirigent protein states, respectively. The rate constant k_{ox} describes the rate of coniferyl alcohol (1) oxidation while k_2 describes the rate of the second coniferyl alcohol radical (2) binding to the DPCA* complex. The binding constants K_1 and K_3 describe the binding of the first coniferyl alcohol radical to the DP and the release of the (+)-pinoresinol (4a) product from the dirigent protein,

respectively, with corresponding forward, k_1 and k_3 , and reverse, k_{-1} and k_{-3} , rate constants.

Numerical simulations (using MathCad7; see Materials and Methods) based on this model were found to give excellent fits to the available data (Figure 6, solid line, overall relative mean square deviation of the observed data to the expected model data was 11.4%).

Moreover, this relatively simple and robust kinetic model adequately explains the observed kinetic behavior of the DP to produce the observed (+)-pinoresinol (4a) in enantiomeric excess in response to changes in DP and coniferyl alcohol radical (2) concentrations. The expected model data are displayed in Figure 6 as solid lines. The fits suggest that binding of CA* (2) to the DP homodimer is both rapid and strong, as expected from the necessity to compete with coupling in free solution. For the CA* (2) bound first (to the unoccupied complex), K_1 was estimated at 10 nM, with k_1 of $\sim 1.7 \times 10^8 \text{ s}^{-1}$, while the binding of the second CA* (2) was best modeled by an essentially irreversible step with $k_2 \sim 2.1 \times 10^8 \text{ s}^{-1}$. The product of the rate constants for coupling and release of the (+)-pinoresinol (4a) product was also estimated to be slow, $k_3 \sim 0.27 \text{ s}^{-1}$ ($K_3 \sim 1.9$), i.e., near the measured k_{fwd} of $0.26 \pm 3 \text{ s}^{-1}$ per dimer at 30 °C (0.15 per dimer at 15 °C; Figures 4A and 6).

Conversion rates were measured under pseudolinear conditions, i.e., during the first 20% of the decay curves, where [CA] (1) remained in excess, and steady-state kinetics can be assumed. To simplify the analysis, it is also assumed that a number of reactions are essentially irreversible including oxidation of coniferyl alcohol (1), coniferyl alcohol radical (2) coupling, and formation of phenols from quinone–methide intermediates. As is apparent from the binding experiments (Figure 2), CA (1) interacts only weakly with the DP, and hence this interaction is ignored in the present model.

Among the models which were not fit by simulations (and thus likely do not operate) were first-order models requiring only the oxidation of a single coniferyl alcohol (1). This is supported by the work of Hapiot et al. (15), who demonstrated that the overall reaction is second order with respect to [CA*] (2). We were also unable to fit the data to models employing binding of CA* (2) to DP monomers with subsequent DP–CA* dimerization.

Nevertheless, since the reaction is performed in a solution with excess coniferyl alcohol (1) present in solution (4 mM), the binding constant, K_D of $370 \pm 65 \mu\text{M}$, would indicate that most of the DP will have coniferyl alcohol (1) weakly bound. Several more complex binding reactions are possible, including reactions involving oxidation of a DP-bound coniferyl alcohol (1) or using a DP-bound coniferyl alcohol anion, i.e., either by action of a one-electron oxidant/oxidase or through radical transfer from an open solution CA* (2) to the bound coniferyl alcohol (1) or its anion. Our current working model described below should thus be viewed as the simplest testable hypothesis.

This slow post-CA* (2) binding and turnover rate results in the observed saturation behavior of the DP and, as mentioned above, could result either from slow coupling of CA* (2) within the DP homodimer or via a slow product release. At first glance, CA* (2) would appear to be too reactive to survive over the second time range. However, there are many well-characterized examples of thermody-

namic stabilization of reactive intermediates by tight, specific, binding, leading to quite long lifetimes. Appropriate examples are the semiquinone radical intermediates of key respiratory and photosynthetic electron transfer pathways. When free in solution, the stability constant (K_s) for ubisemiquinone or plastosemiquinone is quite small, on the order of 10^{-10} M^{-1} (25), the free semiquinone disproportionating under physiological conditions at diffusion-limited rates (26, 27). However, when appropriately bound within active sites, e.g., the Q_B site of bacterial reaction centers or photosystem II or the Q_i site of the cytochrome bc_1 complex, semiquinones can be quite stable, with lifetimes in the seconds to hours (28, 29). Such a thermodynamically stabilized CA^{\bullet} (2) species would necessarily have a lower driving force for coupling, at least within the binding site, possibly accounting for the slow overall reaction. Thus, we cannot rule out the possibility that the DP homodimer stabilizes CA^{\bullet} (2) at its two active sites. This possibility will be investigated in future work since long-lived CA^{\bullet} (2) species should have well-defined spectroscopic signatures, measurable with, e.g., EPR or UV/vis spectroscopy. Indeed, CA^{\bullet} (2) stabilization would require a quite specific and tight binding site on the DP, even though there appears to be no direct catalytic benefit from its stabilization.

Alternatively, processes after CA^{\bullet} (2) coupling could limit DP turnover. This would imply that the quinone–methide intermediate is tightly bound to the DP homodimer, so that either its off rate is close to k_{fwd} or it must be cyclized to (+)-pinoresinol (4a) to be released. If the rate constant for formation of the 8–8' product from the bis(quinone–methide) intermediate in open solution is as slow as suggested by the aggregate rate of cyclization (16), i.e., $k_{phenol} \sim 5.78 \times 10^{-3} \text{ s}^{-1}$ at 23 °C, then two possibilities emerge. First, the 8–8' bis(quinone–methide) is released and accumulates in the steady state (since $k_{phenol} \ll k_{fwd}$). However, because our current assay procedure takes several hours, we would not have detected this accumulation. On the other hand, (+)-pinoresinol (4a) might be the product released from the DP homodimer. In this case, the DP may, in addition to its function in guiding radical–radical coupling, catalyze the cyclization, making $k_{phenol} \geq k_{fwd}$. Furthermore, since we found no effects on overall DP-mediated coupling rates upon addition of excess (+)-pinoresinol (4a) (data not shown), we conclude that the release of (+)-pinoresinol (4a) would be essentially irreversible. Future work will clarify further the precise nature of the reaction mechanism.

ACKNOWLEDGMENT

The authors thank Fabian Maldonado for assistance in protein purification and Michael G. Paice for the gift of a *T. versicolor* laccase sample.

REFERENCES

- Lewis, N. G., and Davin, L. B. (1999) Lignans: biosynthesis and function, in *Comprehensive Natural Products Chemistry* (Barton, D. H. R., Nakanishi, K., and Meth-Cohn, O., Eds.) pp 639–712, Elsevier, London.
- Davin, L. B., Wang, H.-B., Crowell, A. L., Bedgar, D. L., Martin, D. M., Sarkanen, S., and Lewis, N. G. (1997) Stereoselective bimolecular phenoxy radical coupling by an auxiliary (dirigent) protein without an active center, *Science* 275, 362–366.
- Gang, D. R., Costa, M. A., Fujita, M., Dinkova-Kostova, A. T., Wang, H.-B., Burlat, V., Martin, W., Sarkanen, S., Davin, L. B., and Lewis, N. G. (1999) Regiochemical control of monolignol radical coupling: A new paradigm for lignin and lignan biosynthesis, *Chem. Biol.* 6, 143–151.
- Burlat, V., Kwon, M., Davin, L. B., and Lewis, N. G. (2001) Dirigent Proteins and Dirigent Sites in Lignifying Tissues, *Phytochemistry* 57, 883–897.
- Halls, S. C., and Lewis, N. G. (2002) Secondary and quaternary structures of the (+)-pinoresinol forming dirigent protein, *Biochemistry* 41, 9455–9461.
- Culley, D. E., Horovitz, D., and Hadwiger, L. A. (1995) Molecular characterization of disease-resistance response gene *DRR206-d* from *Pisum sativum* (L.), *Plant Physiol.* 107, 301–302.
- Choi, J. J., Klosterman, S. J., and Hadwiger, L. A. (2001) A comparison of the effects of DNA-damaging agents and biotic elicitors on the induction of plant defense genes, nuclear distortion, and cell death, *Plant Physiol.* 125, 752–762.
- Schreier, P., Garbers, C., Langen, G., and Kiedrowski, S. (1999) Tobacco cDNAs for genes induced upon pathogen infection and their uses, Patent DE 19813048.
- Davin, L. B., and Lewis, N. G. (2000) Dirigent proteins and dirigent sites explain the mystery of specificity of radical precursor coupling in lignan and lignin biosynthesis, *Plant Physiol.* 123, 453–461.
- Wang, C.-Z., Davin, L. B., and Lewis, N. G. (2001) Stereoselective phenolic coupling in *Blechnum spicant*: formation of 8–2' linked (–)-*cis*-blechnic, (–)-*trans*-blechnic and (–)-brainic acids, *J. Chem. Soc., Chem. Commun.*, 113–114.
- Davin, L. B., Wang, C.-Z., Helms, G. L., and Lewis, N. G. (2003) [^{13}C]-Specific labeling of 8–2' linked (–)-*cis*-blechnic, (–)-*trans*-blechnic and (–)-brainic acids in the fern *Blechnum spicant*, *Phytochemistry* 62, 501–511.
- Nose, M., Bernards, M. A., Furlan, M., Zajicek, J., Eberhardt, T. L., and Lewis, N. G. (1995) Towards the specification of consecutive steps in macromolecular lignin assembly, *Phytochemistry* 39, 71–79.
- Bernards, M. A., Lopez, M. L., Zajicek, J., and Lewis, N. G. (1995) Hydroxycinnamic acid-derived polymers constitute the polyaromatic domain of suberin, *J. Biol. Chem.* 270, 7382–7386.
- Bu'Lock, J. D., Leeming, P. R., and Smith, H. G. (1962) Pyrones. Part II. Hispidin, a new pigment and precursor of a fungus "lignin", *J. Chem. Soc.* 2085–2089.
- Hapiot, P., Pinson, J., Francesch, C., Mhamdi, F., Rolando, C., and Schneider, S. (1994) Mechanism of oxidative coupling of coniferyl alcohol, *Phytochemistry* 36, 1013–1020.
- Radotic, K., Zakrzewska, J., Sladic, D., and Jeremic, M. (1997) Study of photochemical reactions of coniferyl alcohol. I. Mechanism and intermediate products of UV radiation-induced polymerization of coniferyl alcohol, *Photochem. Photobiol.* 65, 284–291.
- Hapiot, P., Pinson, J., Francesch, C., Mhamdi, F., Rolando, C., and Schneider, S. (1992) One-electron redox potentials for the oxidation of coniferyl alcohol and analogues, *J. Electroanal. Chem.* 328, 327–331.
- Bourbonnais, R., Paice, M. G., Reid, I. D., Lanthier, P., and Yaguchi, M. (1995) Lignin oxidation by laccase isozymes from *Trametes versicolor* and role of the mediator 2,2'-azinobis (3-ethylbenzthiazoline-6-sulfonate) in kraft lignin depolymerization, *Appl. Environ. Microbiol.* 61, 1876–1880.
- Neuhoff, V., Kiel, F., and Schuett, E., Jr. (1972) Small-volume dialyzer, Patent DE 2039051.
- Scatchard, G. (1949) The attraction of proteins for small molecules and ions, *Ann. N.Y. Acad. Sci.* 51, 660–672.
- Gaille, C., Kast, P., and Haas, D. (2002) Salicylate biosynthesis in *Pseudomonas aeruginosa*. Purification and characterization of PchB, a novel bifunctional enzyme displaying isochorismate pyruvate-lyase and chorismate mutase activities, *J. Biol. Chem.* 277, 21768–21775.
- Fenoll, L. G., Rodríguez-López, J. N., García-Molina, F., García-Cánovas, F., and Tudela, J. (2002) Michaelis constants of mushroom tyrosinase with respect to oxygen in the presence of monophenols and diphenols, *Int. J. Biochem. Cell Biol.* 34, 332–336.

23. Lindqvist, A., and Andersson, S. (2002) Biochemical properties of purified recombinant human β -carotene 15,15'-monooxygenase, *J. Biol. Chem.* 277, 23942–23948.
24. Rahman, M. M. A., Dewick, P. M., Jackson, D. E., and Lucas, J. A. (1990) Lignans of *Forsythia intermedia*, *Phytochemistry* 29, 1971–1980.
25. Rich, P. (1982) A physicochemical model of quinone-cytochrome bc complex electron transfers, in *Function of Quinones in Energy Conserving Systems* (Trumpower, B. L., Ed.) pp 73–83, Academic Press, New York.
26. Elliot, A. J., Egan, K. L., and Wan, J. K. S. (1978) Effect of viscosity on the bimolecular termination rate constant for semi-quinone radicals in solution: A kinetic ESR study, *J. Chem. Soc., Faraday Trans. 1* 74, 2111–2120.
27. Wong, S. K., Sytnyk, W., and Wan, J. K. S. (1972) Electron spin resonance study of the self-disproportionation of some semi-quinone radicals in solution, *Can. J. Chem.* 50, 3052–3057.
28. Wraight, C. A. (1982) The involvement of stable semiquinones in the two-electron gates of plant and bacterial photosystems, in *Function of Quinones in Energy Conserving Systems* (Trumpower, B. L., Ed.) pp 181–198, Academic Press, New York.
29. Crofts, A. R., and Berry, E. A. (1998) Structure and function of the cytochrome bc₁ complex of mitochondria and photosynthetic bacteria, *Curr. Opin. Struct. Biol.* 8, 501–509.

BI035959O